On-chip light sheet illumination enables diagnostic size and concentration measurements of membrane vesicles in biofluids

Hendrik Deschout[1,2], Koen Raemdonck[1], Stephan Stremersch[1], Pietro Maoddi[3], Guillaume Mernier[3], Philippe Renaud[3], Sébastien Jiguet[3], An Hendrix[4], Marc Bracke[4], Rudy Van den Broecke[5], Magnus Röding[6], Mats Rudemo[6], Jo Demeester[1], Stefaan C. De Smedt[1], Filip Strubbe[7], Kristiaan Neyts[7], Kevin Braeckmans[1,2,]*

[1]Laboratory of General Biochemistry and Physical Pharmacy, Ghent University, Belgium
[2]Center for Nano- and Biophotonics, Ghent University, Belgium
[3]Laboratory of Microsystems, Ecole Polytechnique Fédérale de Lausanne, Switzerland
[4]Laboratory of Experimental Cancer Research, Ghent University Hospital, Belgium
[5]Department of Gynaecology, Ghent University Hospital, Belgium
[6]Department of Mathematical Statistics, Chalmers University of Technology, Sweden
[7]Liquid Crystals and Photonics Group, Ghent University, Belgium

*Corresponding author, e-mail: Kevin.Braeckmans@UGent.be

Abstract

Cell-derived membrane vesicles that are released in biofluids, like blood or saliva, are emerging as potential non-invasive biomarkers for diseases, such as cancer. Techniques capable of measuring the size and concentration of membrane vesicles directly in biofluids are urgently needed. Fluorescence Single Particle Tracking microscopy has the potential of doing exactly that, by labelling the membrane vesicles with a fluorescent label and analysing their Brownian motion in the biofluid. However, unbound dye in the biofluid can cause high background intensity that strongly biases the fluorescence Single Particle Tracking size and concentration measurements. While such background can be avoided with light sheet illumination, current set-ups require specialty sample holders that are not compatible with high-throughput diagnostics. Here, a microfluidic chip with integrated light sheet illumination is reported, and accurate fluorescence Single Particle Tracking size and concentration measurements of membrane vesicles in cell culture medium and in interstitial fluid collected from primary human breast tumours are demonstrated.

Introduction

The relation between specific types of cell-derived membrane vesicles (MVs) in body fluids and disease progression, e.g. tumour growth and metastasis, is a topic that receives a lot of attention nowadays [1-6]. The size, origin and concentration of cell-derived MVs could entail clinically relevant signatures with diagnostic and prognostic value [2, 5, 7]. Thus, substantial efforts have gone into evaluating and developing techniques suitable for submicron MV characterization in terms of specificity, size and concentration [8]. Specifically, due to a lack of standardized isolation and purification protocols and in order to avoid manipulation artefacts, techniques capable of performing MV characterization directly in body fluids are urgently needed [2, 9, 10].

Fluorescence Single Particle Tracking (fSPT) was recently shown to be the first technique capable of accurately measuring the size distribution and number concentration of fluorescently labelled nanoparticles in undiluted biofluids, such as whole blood [11, 12]. However, being based on epi-fluorescence microscopy, a limitation of the technique is limited contrast due to fluorescence coming from out-of-focus particles or unbound fluorescent dye, as illustrated in **Figure 1a**. Especially the latter aspect can be problematic for fSPT characterization of MVs that require staining with fluorescent labels targeted against specific membrane markers to detect MV subpopulations. As the concentration of MVs in e.g. a patient sample is unknown a priori, a surplus of labelled antibodies has to be added in order to be certain that all vesicles will be stained. This will typically result in a substantial fraction of unbound fluorescent labels in the sample medium and a concomitant decrease in contrast. Thus, smaller (dimmer) particles are more difficult to detect, resulting in an underestimation of the number concentration and a biased size distribution. This is especially of importance for a correct characterization of the smaller types of MVs, such as exosomes, with a size below 100 nm [10, 13].

To enable high-throughput diagnostics of MVs in biofluids, we created a mass producible microfluidic chip with integrated light sheet illumination for fSPT size and concentration measurements of submicron MVs that are fluorescently labelled directly in the biofluid without the need for isolation or purification steps. Light sheet illumination presents an attractive alternative to conventional epi-illumination as it combines superior contrast with real-time imaging, as is required to capture the MV's fast Brownian motion [14-16]. Although light sheet illumination has mainly been applied to mesoscopic imaging set-ups for developmental biology [17-20], some reports demonstrate its usefulness for high-resolution imaging applications as well [15, 16, 21, 22]. As illustrated in **Figure 1a**, this requires two objective lenses positioned perpendicular to one another in very close proximity, one for creating the light sheet, the other one for imaging. This has been shown to be possible for fSPT experiments in combination with custom made sample holders having two high-quality optical windows for illumination and imaging [14-16]. However, as they are difficult and expensive to manufacture [23], they are not suitable for high-throughput diagnostic assays for which inexpensive disposable sample holders are preferred to avoid extensive cleaning procedures and sample contamination.

Here, we realize for the first time light sheet illumination in a mass-manufacturable microfluidic chip by coupling laser light into a planar waveguide structure in which a microchannel is provided, containing the sample. We show that the contrast with which the

nanospheres can be visualized, improves substantially compared to classic epi-fluorescence illumination, close to what has been achieved on dedicated light sheet microscopes. To demonstrate the potential of the microfluidic chip as a diagnostic tool, fSPT measurements are performed of MVs in cell culture medium and in interstitial fluid collected from primary human breast tumours. Because of the high background intensity coming from unbound marker molecules, the on-chip light sheet illumination is found to be essential for correct MV characterization.

Experimental Section

fSPT size distribution and number concentration measurements

fSPT measurements can be used to determine the number concentration and size distribution of particles undergoing Brownian motion in a dispersion [11, 12]. Briefly, first a movie is recorded of the diffusing particles at a fixed *z*-position and their motion trajectories are determined, using image processing [24]. From the mean square displacement, a diffusion coefficient can be estimated for each individual trajectory. This leads to a distribution of diffusion coefficients when many particles are analysed. A maximum entropy deconvolution step can subsequently be applied to this distribution to reduce sampling noise and improve its precision [11]. The distribution of diffusion coefficients can be converted to a size distribution via the Stokes-Einstein relation. The number concentration can be derived from the trajectories as well, since the particle number in each image is known and the observation volume can be inherently calibrated from the time that particles appear in focus [12]. The fSPT experiments for determination of the size and concentration are performed in a silicon chip. The microchannel is filled with the dispersion of Alexa Fluor 647 labelled MVs, and the objective lens is positioned so that the focal plane coincides with the light sheet. Subsequently, 10 to 20 independent movies of 10 seconds are recorded at randomly chosen locations in the sample, with a frame rate of 22.6-27.6 frames per second, an image acquisition time of 20-30 ms, an image size of 436-450 pixels in the *x*-direction and 124-192 pixels in the *y*-direction, and a pixel size of 196 nm. Particle trajectories from all movies are calculated off line [24], and pooled before calculation of the size distribution and number concentration. Only trajectories of minimally 5 positions are included in the analysis to remove false positives. For both illumination types, the size and concentration results were obtained from one and the same sample.

Chip fabrication process

Multiple microfluidic chips with an integrated planar waveguide are simultaneously fabricated in one process on 10 cm diameter wafers. Two different types of wafers are used, standard silicon wafers and 145 µm thick borosilicate glass wafers. The wafers are first cleaned with an O_2 plasma in a TepPla 300 plasma system. The clean room process is illustrated in **Figure S4**. First, SU-8 type GM 1060 (Gersteltec Sàrl, Switzerland) mixed with 6% of the epoxy resin D.E.R.™ 353 (The Dow Chemical Company, Belgium) is spin coated on the wafer using a Sawatec LSM 200 coater, to obtain a ~25 µm thick bottom cladding layer, followed by soft baking on a Sawatec HP 401 Z hotplate (see **Supporting Table 1**). Next, pure SU-8 type GM 1060 is spin coated on the bottom cladding layer to obtain a ~5 µm

thick core layer, again followed by a soft bake step. Finally, SU-8 type GM 1060 mixed with 6% of the epoxy resin D.E.R.™ 353 is spin coated on the core layer to obtain a ~25 µm thick top cladding layer, followed by a final soft bake step. To create the microfluidics, the whole 3-layer structure is exposed to 270 mJ/cm^2 of the i-line (365 nm) of a Karl Suss MA 6 mask aligner using a Cr mask. Next, the structure is post exposure baked on a programmable hotplate, and developed in a wet bench using propylene glycol methyl ether acetate (PGMEA). The wafer is finally diced with a Disco DAD 321 Automatic Dicing Saw, to obtain separate microfluidic chips that each contain a planar waveguide and microchannel with in- and outlet reservoir.

Isolation, sizing, and labelling of breast cancer cell-line derived MVs

The MCF-7 breast cancer cell line [25] stably transfected with GFP-Rab27B was maintained at 37°C and 5% CO_2 in Dulbecco's Modified Eagle Medium (Invitrogen, Belgium) supplemented with 10% fetal bovine serum (FBS) and penicillin/streptomycin. For MV production, cells were cultured in DMEM supplemented with 10% Exo-FBS™ (System Biosciences, Belgium) for 48 hours. MVs were isolated from the conditioned medium by differential centrifugation. Briefly, conditioned cell culture medium was successively centrifuged at 300 g for 10 minutes, 3000 g for 10 minutes, and 15000 g for 30 minutes and the supernatant was collected after each step. Next, the supernatant was concentrated using a Vivaspin 20 with molecular weight cut-off 50 kDa (Sartorius, Belgium) to a volume of about 5 ml. The MVs were then pelleted by ultracentrifugation (UC) for 70 minutes at 120 000 g, washed with phosphate buffered saline (PBS) and again pelleted by UC at 120 000 g for 70 minutes. Finally the MV pellet was resuspended in 200 µl PBS. After diluting 5× in PBS, the MV size distribution was measured by dynamic light scattering measurements at 25°C on a Nano-ZS (Malvern, UK), see **Figure S5**. The MVs were fluorescently labelled by mixing 3 µl of the isolated MVs with 6 µl HEPES buffer, 1 µl 10× Annexin V binding buffer (100 mM HEPES, 1.4 M NaCl, and 25 mM CaCl2, pH 7.4) and 0.1 µl neat Annexin V Alexa Fluor 647 (Molecular Probes™, Life Technologies Europe, Belgium). The sample was gently mixed and incubated in the dark for 15 minutes at room temperature prior to measurement.

Fluorescent labelling of MVs in tumour interstitial fluid

Primary breast cancer resection specimens were collected at Ghent University Hospital. Written informed consent was obtained from each patient according to the recommendations of the local ethics committee. About 0.25 g of clean fresh tissue was cut into small pieces (1-2 mm^3), washed carefully with PBS, and incubated in 1 ml PBS for 1 hour at 37°C in a humidified CO_2 incubator. The samples were centrifuged [26] at 500 g for 10 minutes and 1500 g for 20 minutes. Without any further purification, 4 µl of the final supernatant (i.e. tumour interstitial fluid) was mixed with 8 µl of Annexin V binding buffer (10 mM HEPES, 140 mM NaCl, and 2.5 mM $CaCl_2$, pH 7.4) and 4 µl of Annexin V Alexa Fluor 647 (Invitrogen, Belgium). The sample was gently mixed and incubated in the dark for 15 minutes at room temperature prior to measurement. Note that size measurements by DLS are not an option due to the high protein content and the presence of other light scattering compounds in interstitial

fluid. Neither does DLS allow to perform concentration measurements, nor can it detect a specific subtype of MVs as can be achieved with fSPT by using labelled antibodies.

Results

Fabrication of the chip

To obtain on-chip light sheet illumination, a mass-manufacturable microfluidic chip was created according to the design illustrated in **Figure 1b**. The chip is fabricated on a glass or silicon substrate on top of which a planar waveguide structure is created consisting of 3 layers of SU-8 that are sequentially deposited by spin coating followed by a soft bake step. The refractive index of the bottom and top layer (~25 µm thickness each) is lowered by mixing the SU-8 with the epoxy resin D.E.R.™ 353, making these layers suitable as waveguide cladding while the middle layer (~5 µm thickness) acts as waveguide core [27]. Finally, a microchannel of 100 µm width containing in- and outlet reservoirs is created in the SU-8 waveguide using standard photolithography (see **Figure 2a,b**). The entire process is carried out on a 10 cm diameter wafer, thus obtaining 20 chips in parallel after dicing. Chips based on the glass substrate are covered with a polydimethylsiloxane (PDMS) block to seal the microchannel and to provide in and outlets for the sample (see **Figure 2c**). Imaging of the sample is then performed through the 145 µm thick glass substrate. Chips based on the silicon substrate are covered with a microscopy cover slip containing a thin layer of PDMS through which the sample in the microchannel can be imaged (see **Figure 2d**). The chips are mounted on a fluorescence microscope for image acquisition of the diffusing nanoparticles. Laser light of 640 nm is coupled into the waveguide using an optical fiber attached to a high precision alignment stage (see **Supporting Information**).

Characterization of the light sheet

Simulations of the fundamental propagating light mode show that such a planar waveguide is capable of producing a light sheet with a fairly uniform thickness over a large field of view, with a full width at half maximum (FWHM) of 4.6 µm at the waveguide exit, diverging to 7.5 µm over a distance of 100 µm (see **Supporting Information**). The actual light sheet of both types of chips was characterized by acquiring a *z*-stack through the microchannel containing a dispersion of 0.2 µm fluorescent polystyrene nanospheres (for details, see Supporting Information). The light sheet intensity profile along the optical axis (i.e. perpendicular to the sheet of light) was calculated from the average intensity of the nanospheres visible in each frame of the *z*-stack (see **Supporting Video 1**). The average intensity profile across the entire microchannel width is shown in **Figure 3a**, resulting in an average thickness of ~9 µm FWHM. The smaller intensity peaks visible in the intensity profiles indicate that the waveguide is likely multimodal which could explain the slight difference with the theoretical calculations.

Determining the contrast improvement

The aim of light sheet illumination is to improve the contrast, which was quantified for both chips according to $(I_p - I_b)/(I_p + I_b)$, with I_p the intensity of the nanoparticle and I_b the average

local background intensity [14]. The microchannel was filled with a dispersion of 0.2 µm fluorescent polystyrene nanospheres containing various amounts of Cy5 dye to simulate different background intensities coming from free dye. As shown in **Figure 3b**, compared to classic epi-illumination, a contrast improvement of 1.5 - 2.4× was obtained in the glass chip, and 1.9 - 6.4× in the silicon chip, depending on the background intensity (see **Supporting Information**). This improvement approaches the performance of light sheet illumination as created with a high quality objective lens (see **Figure 1a**) [14]. The better relative increase in contrast with the silicon chip is due to the light intensity almost going to zero at the edges of the light sheet, which is not the case for the glass chip (cfr. **Figure 3a**). However, in absolute terms the glass chip produced the best contrast as the silicon chip suffers from a higher background intensity due to the reflectivity of the silicon substrate (i.e. a doubling of the background intensity).

Size and concentration measurements of cell-derived MVs

In a next step, on-chip fSPT size and concentration measurements were performed of cell-derived MVs isolated from the conditioned cell culture medium of breast cancer cells [28] (see **Supporting Video 2**). An excess of fluorescently labelled Annexin V was used to label the cell-derived MVs which are known to expose phosphatidylserine (PS) on their surface [13], followed by on-chip fSPT analysis without additional purification. As shown in **Figure 4a**, using sheet illumination, the majority of the MVs were situated in the 50 - 700 nm size range (in agreement with dynamic light scattering), and the overall number concentration was $8.4 \cdot 10^8$ #/ml. Using conventional epi-fluorescence, a 4× lower concentration of only $1.9 \cdot 10^8$ #/ml was found with a size distribution that is clearly shifted towards larger values.

To demonstrate the potential of the microfluidic chip with integrated planar waveguide as a diagnostic tool, fSPT measurements were performed on cell-derived MVs secreted in the interstitial fluid harvested from fresh human breast cancer specimens [26]. To ensure optimal fluorescent labelling of PS-exposing MVs present in the interstitial fluid, again an excess of dye-conjugated Annexin V was added. Subsequent on-chip fSPT analysis was performed without any additional purification steps to remove unbound label. A broad distribution of cell-derived MV sizes was found in the interstitial fluid, as shown in **Figure 4b**. The majority of the MVs are situated in the 90 - 900 nm size range, with a total number concentration of $4.1 \cdot 10^8$ #/ml. Using conventional epi-fluorescence the background fluorescence was so high that only very few MVs were visible and no meaningful size distribution or concentration could be determined. This once more clearly demonstrates that improving contrast by light sheet illumination is essential for correct MV characterization, especially when there is a high background intensity due to out of focus particles and unbound fluorescent dye.

Discussion and conclusion

Here, we have produced a mass-manufacturable microfluidic chip with integrated light sheet illumination, and successfully demonstrated that it allows accurate fSPT size and concentration measurements of MVs in cell culture medium and in interstitial fluid collected from primary human breast tumours. The on-chip light sheet illumination was shown to allow

visualization of the small and dim MVs that are missed by the significant background present in conventional epi-fluorescence illumination.

Nonetheless, further optimization of the chip's performance should be possible. Based on the simulated light sheet created by the fundamental propagating light mode, it seems that at least 30% reduction of the light sheet thickness should be possible by reducing the core thickness and fine-tuning of the refractive indices of core and cladding layers so as to obtain a monomodal waveguide. This requires optimization of the fabrication process, including the amount of D.E.R.™ 353 in the cladding layers, spin coating speeds, and baking times. In case of the silicon chip, contrast could be further improved by applying a non-reflective coating (e.g. black SU-8 formulations) on the silicon wafer before spin coating of the waveguide structure. Furthermore, automation of the coupling of light from the fiber into the waveguide is expected to make the chip more suitable for high-throughput measurements.

Interestingly, one other type of microfluidic chip was recently reported for MV characterization in biological fluids based on labelling with magnetic nanoparticles and miniaturized nuclear magnetic resonance detection [7]. Although it was shown to be capable of discriminating different types of MVs with high sensitivity, it does not feature independent size and concentration measurements. In contrast, the microfluidic chip presented here is much simpler in design, can be mass-fabricated at a low cost, and allows at the same time MV identification, as well as size and concentration measurements. Thus, it opens the possibility to be used as a diagnostic tool that combine low cost, ease of use, and sensitivity [29, 30].

Acknowledgements

H. Deschout would like to acknowledge the financial support of the Agency for Innovation by Science and Technology in Belgium. Financial support by the Ghent University Special Research Fund and the Fund for Scientific Research Flanders (FWO, Belgium) is acknowledged with gratitude. The authors thank S. Verstuyft and D. Van Thourhout for their help in the chip fabrication process.

References

1. K. Al-Nedawi, B. Meehan and J. Rak, *Cell Cycle*, 2009, **8**, 2014-2018.
2. C. D'Souza-Schorey and J. W. Clancy, *Gene Dev*, 2012, **26**, 1287-1299.
3. F. Fleissner, Y. Goerzig, A. Haverich and T. Thum, *Am J Transplant*, 2012, **12**, 289-297.
4. T. H. Lee, E. D'Asti, N. Magnus, K. Al-Nedawi, B. Meehan and J. Rak, *Semin Immunopathol*, 2011, **33**, 455-467.
5. V. Muralidharan-Chari, J. W. Clancy, A. Sedgwick and C. D'Souza-Schorey, *J Cell Sci*, 2010, **123**, 1603-1611.
6. J. Skog, T. Wurdinger, S. van Rijn, D. H. Meijer, L. Gainche, M. Sena-Esteves, W. T. Curry, B. S. Carter, A. M. Krichevsky and X. O. Breakefield, *Nat Cell Biol*, 2008, **10**, 1470-U1209.
7. H. L. Shao, J. Chung, L. Balaj, A. Charest, D. D. Bigner, B. S. Carter, F. H. Hochberg, X. O. Breakefield, R. Weissleder and H. Lee, *Nat Med*, 2012, **18**, 1835-+.
8. E. van der Pol, A. G. Hoekstra, A. Sturk, C. Otto, T. G. van Leeuwen and R. Nieuwland, *J Thromb Haemost*, 2010, **8**, 2596-2607.

9. B. Gyorgy, T. G. Szabo, L. Turiak, M. Wright, P. Herczeg, Z. Ledeczi, A. Kittel, A. Polgar, K. Toth, B. Derfalvi, G. Zelenak, I. Borocz, B. Carr, G. Nagy, K. Vekey, S. Gay, A. Falus and E. I. Buzas, *Plos One*, 2012, **7**.
10. E. van der Pol, A. N. Boing, P. Harrison, A. Sturk and R. Nieuwland, *Pharmacol Rev*, 2012, **64**, 676-705.
11. K. Braeckmans, K. Buyens, W. Bouquet, C. Vervaet, P. Joye, F. De Vos, L. Plawinski, L. Doeuvre, E. Angles-Cano, N. N. Sanders, J. Demeester and S. C. De Smedt, *Nano Lett*, 2010, **10**, 4435-4442.
12. M. Roding, H. Deschout, K. Braeckmans and M. Rudemo, *Phys Rev E*, 2011, **84**.
13. C. Thery, M. Ostrowski and E. Segura, *Nat Rev Immunol*, 2009, **9**, 581-593.
14. J. G. Ritter, R. Veith, J. P. Siebrasse and U. Kubitscheck, *Opt Express*, 2008, **16**, 7142-7160.
15. J. G. Ritter, R. Veith, A. Veenendaal, J. P. Siebrasse and U. Kubitscheck, *Plos One*, 2010, **5**.
16. J. H. Spille, T. Kaminski, H. P. Konigshoven and U. Kubitscheck, *Opt Express*, 2012, **20**, 19697-19707.
17. J. Huisken and D. Y. R. Stainier, *Development*, 2009, **136**, 1963-1975.
18. J. Huisken, J. Swoger, F. Del Bene, J. Wittbrodt and E. H. K. Stelzer, *Science*, 2004, **305**, 1007-1009.
19. P. J. Keller, A. D. Schmidt, A. Santella, K. Khairy, Z. R. Bao, J. Wittbrodt and E. H. K. Stelzer, *Nat Methods*, 2010, **7**, 637-U655.
20. P. J. Keller, A. D. Schmidt, J. Wittbrodt and E. H. K. Stelzer, *Science*, 2008, **322**, 1065-1069.
21. F. Cella Zanacchi, Z. Lavagnino, M. P. Donnorso, A. Del Bue, L. Furia, M. Faretta and A. Diaspro, *Nat Methods*, 2011, **8**, 1047-1049.
22. T. A. Planchon, L. Gao, D. E. Milkie, M. W. Davidson, J. A. Galbraith, C. G. Galbraith and E. Betzig, *Nat Methods*, 2011, **8**, 417-U468.
23. F. Cutrale and E. Gratton, *Microsc Res Techniq*, 2012, **75**, 1461-1466.
24. K. Braeckmans, D. Vercauteren, J. Demeester and S. C. De Smedt, in *Nanoscopy and Multidimensional Optical Fluorescence Microscopy*, ed. A. Diaspro, CRC Press / Taylor & Francis Group, Boca Raton, 2010.
25. A. Hendrix, W. Westbroek, M. Bracke and O. De Wever, *Cancer Res*, 2010, **70**, 9533-9537.
26. A. De Boeck, P. Pauwels, K. Hensen, J. L. Rummens, W. Westbroek, A. Hendrix, D. Maynard, H. Denys, K. Lambein, G. Braems, C. Gespach, M. Bracke and O. De Wever, *Gut*, 2013, **62**, 550-560.
27. J. M. Ruano-Lopez, M. Aguirregabiria, M. Tijero, M. T. Arroyo, J. Elizalde, J. Berganzo, I. Aranburu, F. J. Blanco and K. Mayora, *Sensor Actuat B-Chem*, 2006, **114**, 542-551.
28. A. Hendrix, D. Maynard, P. Pauwels, G. Braems, H. Denys, R. Van den Broecke, J. Lambert, S. Van Belle, V. Cocquyt, C. Gespach, M. Bracke, M. C. Seabra, W. A. Gahl, O. De Wever and W. Westbroek, *J Natl Cancer I*, 2010, **102**, 866-880.
29. K. K. Ghosh, L. D. Burns, E. D. Cocker, A. Nimmerjahn, Y. Ziv, A. El Gamal and M. J. Schnitzer, *Nat Methods*, 2011, **8**, 871-U147.
30. H. Y. Zhu, S. O. Isikman, O. Mudanyali, A. Greenbaum and A. Ozcan, *Lab Chip*, 2013, **13**, 51-67.

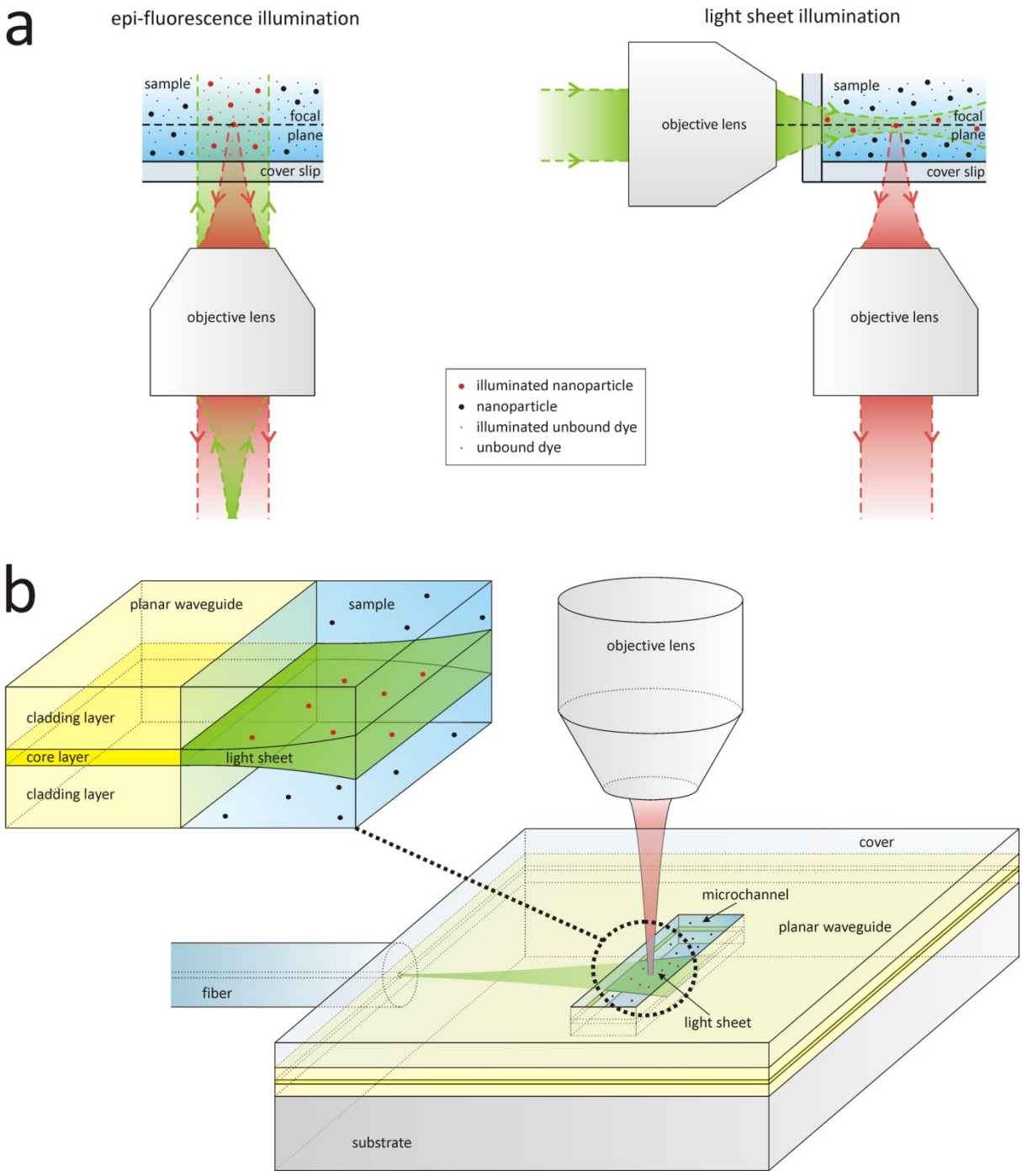

Figure 1. Microfluidic chip with integrated waveguide for light sheet illumination. a) Illustration of the (green) excitation and (red) fluorescence light path in epi-fluorescence and light sheet illumination. The contrast for the nanoparticles in focus is better with light sheet illumination because the nanoparticles and unbound dye out of focus are not illuminated. b) Design of microfluidic chip with integrated waveguide for on-chip light sheet illumination. Laser light enters the planar waveguide by means of an optical fiber. While the laser light is confined in the vertical direction, it can spread horizontally in the waveguide so that a sheet of light emerges in the microchannel. The fluorescence light is collected by an objective lens whose focal plane coincides with the light sheet. The drawing is not to scale.

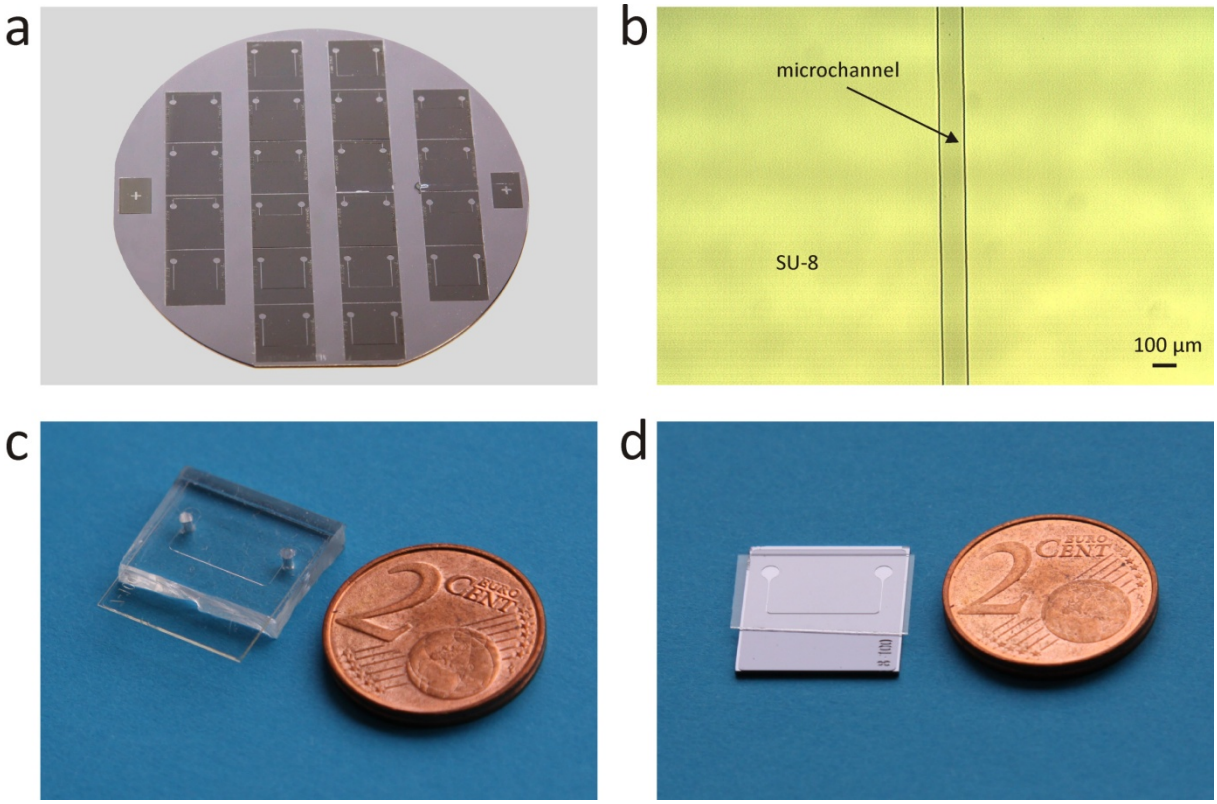

Figure 2. Photographs of the microfluidic chips with planar waveguide for light sheet illumination in a microchannel. a) Image of a silicon wafer with 20 planar waveguides and microchannels made from SU-8 after photolithography. b) Light microscopy image of a microfluidic chip showing the 100 µm wide microchannel. c) Image of microfluidic chip with glass substrate on top of a PDMS block. d) Image of microfluidic chip with silicon substrate covered with a microscope cover slip.

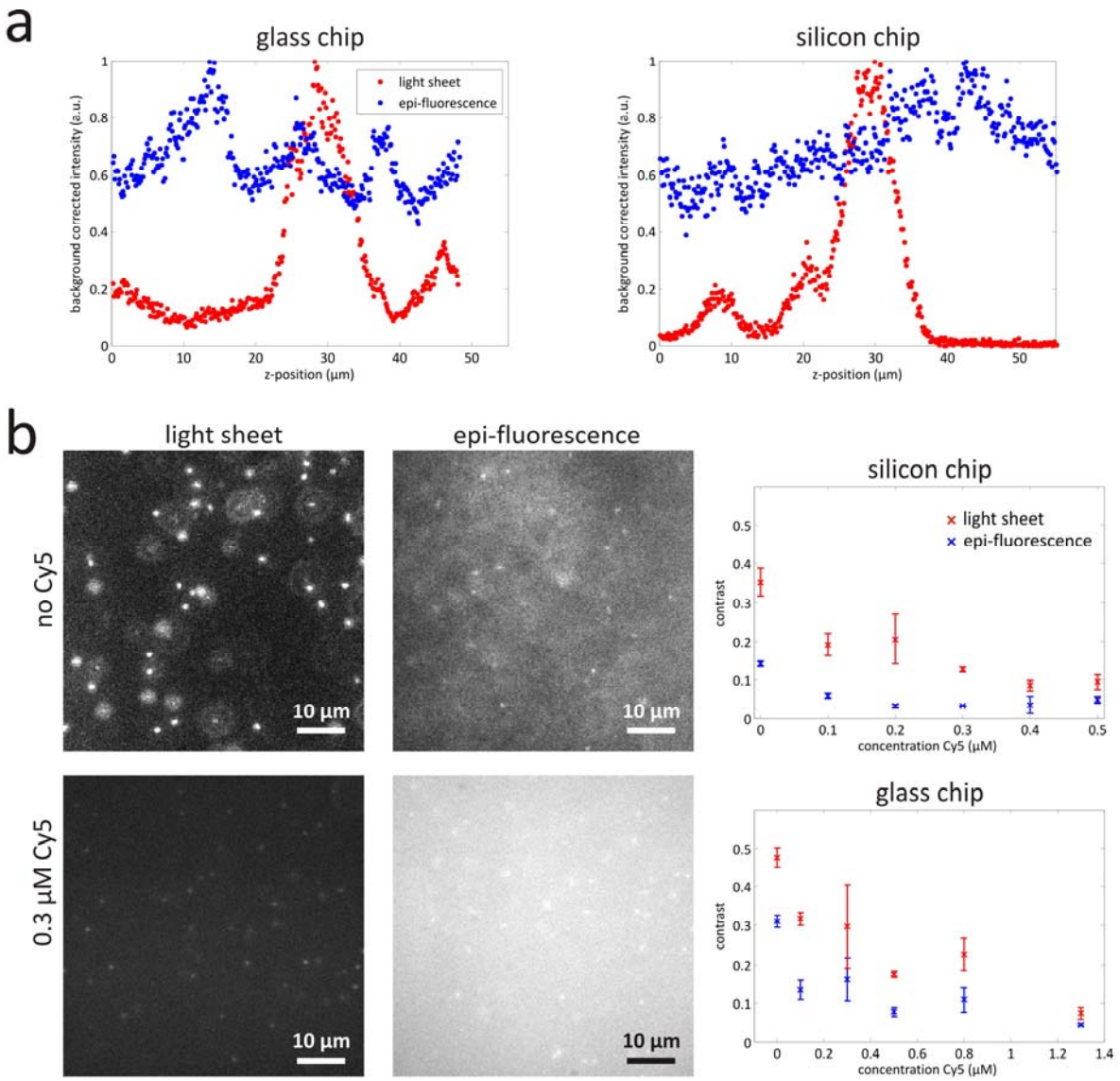

Figure 3. Experimental characterization of the light sheet and contrast. a) Average light sheet intensity profile along the optical axis of the microscope imaging lens. Contrary to epi-fluorescence illumination (blue data points), illumination through the planar waveguide results in excitation light that is restricted to a thin region at the centre of the microchannel with a FWHM of ~9 µm (red data points). b) In order to determine the gain in contrast using light sheet illumination versus epi-fluorescence illumination, the microchannel is filled with a dispersion of 0.2 µm fluorescent polystyrene nanospheres. To mimic different values of background intensity, different concentrations of the red fluorescent dye Cy5 are added. Images are recorded using both illumination modes with the microscope focused at the centre of the light sheet. Example images obtained with a silicon chip are shown to the left. Contrast values for a range of Cy5 concentrations using the silicon and glass chip are shown to the right. The error bars represent the standard deviation.

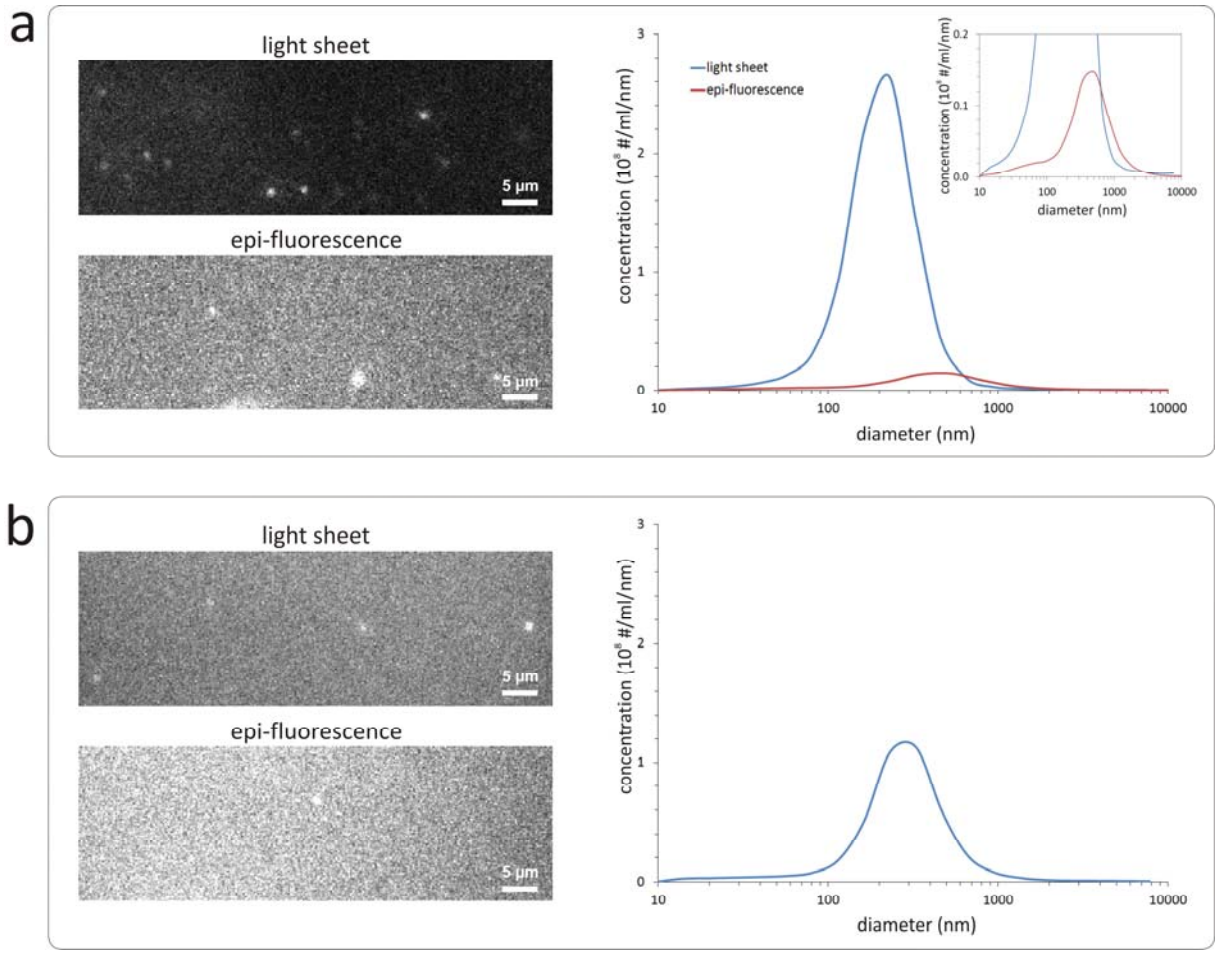

Figure 4. On-chip fSPT concentration and size measurements of cell-derived membrane vesicles. a) fSPT size distribution and number concentration measurements are performed on cell-derived MVs in cell culture medium. The MVs are clearly visible when using light sheet illumination, while only a few particles are visible in conventional epi-fluorescence illumination mode due to the much higher background fluorescence. This results in a 4× underestimation of the number concentration and a bias towards larger (and brighter) MVs for epi-fluorescence illumination versus sheet illumination. b) Similar fSPT experiments are performed on MVs in patient derived interstitial fluid. The MVs are visible when using light sheet illumination, while almost no particles are visible in epi-fluorescence illumination mode. A meaningful concentration and size distribution could only be obtained when using sheet illumination.